Published in final edited form as:
J Memb Sci. 2012 May 15; 401-402: 25–32. doi:10.1016/j.memsci.2012.01.015.

Modulating molecular and nanoparticle transport in flexible polydimethylsiloxane membranes

Kexin Jiao[2], **Chase L. Graham**[1], **Justin Wolff**[2], **Ratnasabapathy G. Iyer**[1], and **Punit Kohli**[2]

Ratnasabapathy G. Iyer: riyer@claflin.edu; Punit Kohli: pkohli@chem.siu.edu

[1]Department of Chemistry, Claflin University, Orangeburg, SC 29115

[2]Department of Chemistry and Biochemistry, Southern Illinois University, Carbondale, IL 62901

Abstract

The ability to fabricate flexible filtration membranes that can selectively separate particles of different sizes is of considerable interest. In this article, we describe a facile, reproducible and simple one-step method to produce pores in polydimethylsiloxane (PDMS) membranes. We embedded micron-sized $NaHCO_3$ particles in 50 micron thick PDMS films. After curing, the membranes were immersed in concentrated HCl acid. Pores were generated in the membrane by the evolution of CO_2 gas from the reaction of $NaHCO_3$ and HCl. High resolution Scanning Electron Microscope images clearly reveal the presence of openings on the surface and the cross-section of the membranes. Fluorescence and back-scattered electron imaging of porous PDMS membrane with embedded gold nanoparticles and comparison with non-porous PDMS membranes provided unambiguous evidence of pores in the membrane. Transport studies of molecular fluoresceinate ions, ions (sodium and chloride) and 240 nm polystyrene nanoparticles through these membranes demonstrate passable pores and existence of channels within the body of the membrane. Mechanically stretching the porous PDMS membrane and comparing the flow rates of fluoresceinate ions and the polystyrene beads through the stretched and unstretched membranes allowed a direct proof of the modulation of transport rate in the membranes. We show that stretching the membranes by 10% increases the flow rate of fluorescein molecules by 2.8 times and by a factor of approximately ~40% for the polystyrene nanoparticles.

Keywords

Modulating transport; Flexible membranes; Polydimethylsiloxane; Nanoparticles; Mechanical stretching

Correspondence to: Ratnasabapathy G. Iyer, riyer@claflin.edu; Punit Kohli, pkohli@chem.siu.edu.

Supporting materials

Figure 1S shows the distribution of $NaHCO_3$ powder in PDMS prepolymer. Figure 2S shows a scanning electron micrograph of a porous membrane in which some of the pores did not contain gold elemental signal (EDX data). An optical photograph of U-tube showing the transport of fluorescein through the membrane is shown in Figure 3S. Figure 4S shows the calibration curve for emission intensity and number of 240 nm particles. Figure 5S shows a schematic of the change in the dimension of the PDMS membrane after stretching of the membrane.

Introduction

Polymer filtration membranes are of great interest due to their potential applications in drug delivery,[1,2] biomolecule separation,[3,4] water and air purification,[5] biological and chemical sensing,[6–9] battery separators,[10] fuel cells,[11] and catalysis.[12] Various polymer membranes with narrowly distributed pore sizes ranging from the nano to micron-scale have been prepared using myriad techniques such as track-etching, selectively etching block copolymers, reverse templating etc.[13–15] For processes requiring multiple filtration steps, such as purification of water that involves microfiltration, ultrafiltration and nanofiltration, multiple membranes with steadily decreasing pore sizes are required. Manipulating the pore size of the membranes chemically through grafting of other molecules on the surface of the pores or by modifying the size of particles to be filtered through ligation are some of the methods used for adjusting transport properties through the membranes.[16–18] Such modifications, however, lead to a slow through-put, are expensive and can harm the integrity of the polymer membrane. Another method described in the literature is the use of electric-field for modulating the transport of molecules through the membranes.[19–26] Therefore, flexible and robust porous membranes that can withstand considerable stress forces and allow tuning of the transport rate without the need for costly and time-consuming changes, are very attractive for scientific and industrial applications

Polydimethylsiloxane (PDMS) is particularly interesting as a membrane material due to its chemical stability, non-toxicity, transparency and ability to be manipulated.[27] PDMS is the material of choice for use in microfluidic devices, microcontact printing etc.[28,29] If one were able to produce pores in PDMS, the high flexibility and mechanical strength of PDMS would accord adjustable pore sizes simply through mechanical stretching. A porous PDMS membrane thus has the potential to be a size-selective filter. However, to date very little effort has been expended towards this goal.[30–32]

Here we describe a simple one-pot and inexpensive method for generating pores in cured PDMS *via in-situ* chemical reactions. The reaction of $NaHCO_3$ and HCl produced water and CO_2, the expulsion of which formed pores within the PDMS films.

To the best of our knowledge, this is the first report of generating pores *in-situ* chemically in cured PDMS using a simple one-pot method for the purpose of exploiting the flexibility of PDMS for size-selective filtration. Pore-formation in polymer membrane using a similar method was recently published while our manuscript was under review.[33] However, that manuscript dealt with a different polymer and a different source of carbonate species was used. A schematic diagram showing the changes in the pores shape and dimensions with stretching of the membrane is shown in Figure 1. Evidence of adjustable pore sizes was obtained by studying the transportation rates of fluorescein solution and fluorescent 240 nm polystyrene nanoparticles through the stretched and unstretched membranes. We demonstrate that the transport of molecules and nanoparticles can be modulated with mechanical stretching. The fluorescein transport rate was increased ~2.8 times and that of polystyrene by 40% after stretching the membrane by 10%

Experimental

Materials

Sylgard 184 and a curing agent were purchased from Dow Corning; $NaHCO_3$ and concentrated HCl were purchased from Fisher Scientific; Triton X-100 was purchased from United States Biochemical Corporation; Sodium Fluoresceinate was purchased from Eastman Chemical Company; and 240 nm fluorescent nile-red impregnated polystyrene solution was purchased from Spherotech Inc.

Membrane synthesis

The PDMS film was synthesized from a prepolymer of 10:1 ratio of silicone elastomer (Sylgard 184) and curing agent respectively. Finely powdered $NaHCO_3$ (7.5% – 17.5% of the total mass of the prepolymer) was simultaneously mixed with the prepolymer. A spincoater was used to control the thickness of the PDMS membranes using a defined spin rate. The resultant PDMS films were cured in a drying oven at 110 °C and were then placed in concentrated HCl for 1–3 hours. As PDMS is hydrophobic, a few drops of surfactant (Triton X-100) were also added to promote the permeation of the HCl solution into the as-made PDMS films. Bubbles were observed during this process, indicating that CO_2 was released from the reaction of HCl with the embedded $NaHCO_3$. After removal from HCl, the membranes were washed thoroughly with water and ethanol and air-dried. Cold cured PDMS membrane was prepared in the similar way but was cured at room temperature prior to treatment with concentrated HCl over night.

Scanning Electron Microscopy (SEM)

SEM images of the PDMS membranes were obtained on a FEI Quanta 450 equipped backscattering and secondary electron detectors and on a Hitachi 570. The membranes were mounted on a carbon tape affixed to an aluminum stub and sputter-coated with Au/Pd prior to loading in the SEM.

Energy Dispersed X-ray analysis (EDX)

EDX analyses of the PDMS membranes were obtained using an Oxford detector attached to a FEI Quanta 450. The membranes were soaked in a solution containing gold nanoparticles (GNPs), and were then thoroughly rinsed and dried in air. A conductive coating of carbon was applied prior to EDX analysis. Gold nanoparticles were synthesized using the method described by Macfarland et al. with particles diameter of ~13 nm.[35] These experiments were performed to gain information on internal morphology of the membranes.

Inverted Fluorescence Microscopy (IFM) analysis

IFM images were obtained on a LEICA DM IRB equipped with a QImage (Cooled Mono 12-bit) CCD camera. IFM analysis was performed on two membranes: one PDMS film without $NaHCO_3$ in it and another membrane that contained $NaHCO_3$ and was treated with HCl. All the membranes were soaked in a 0.4% w/v solution of nile-red containing 240 nm polystyrene particles. A 41004 Texas Red filter (exciting and emitting band widths of the filter used were 527–567 nm and 605–682 nm, respectively) was used for capturing the fluorescent images with a CCD camera.

UV-Vis Spectroscopy

UV-Vis spectra were recorded on a Perkin-Elmer Lambda 25 spectrophotometer (slit width = 1 nm). 5 mL of a 10 μM sodium fluoresceinate solution was placed in one arm of a U-tube. The other arm was filled with 5 mL of water. The porous PDMS membrane was sandwiched between the two arms and held in place using a clamp. Spectra were recorded every 10 minutes for 100 minutes. For measurements using 240 nm polystyrene 6 particles, 200 μL of 1% w/v solution of the polystyrene particles was diluted to 5 mL, resulting in a 0.04% w/v solution, and poured into one arm of the U-tube along with a magnetic stir bar. On the other arm, 3 mL of water was taken. The U-tube was placed on a magnetic stirrer and spectra were recorded every 10 minutes for 120 minutes.

Results and Discussion

A. Synthesis, characterization and morphology of pores in the films

We employed porous PDMS to demonstrate modulation of molecular transport by applying stress on the membranes. $NaHCO_3$ particles with sizes varying from 2 to 30 μm were evenly dispersed in PDMS prepolymer (Figure 1S) and cured within the polymer matrix. The cured film with embedded $NaHCO_3$ was then immersed in concentrated HCl. The reaction between $NaHCO_3$ and HCl liberated CO_2 and H_2O which passed through the membrane creating pores in the film. H_2O from this reaction can also react with Si-H to produce H_2 which can contribute to creating the pores in the film.[34] But the contribution of SiH/water reaction to the overall pore formation is expected to be minimum because SiH content in the polymer is insignificant as compared to $NaHCO_3$ present in the polymer and that SiH/water reaction is also present in the control membrane (prepared with no $NaHCO_3$ and treated with HCl) but did not show the presence of pores in it. Thus, we attribute evolution of gaseous products in the fabrication of porous PDMS membrane. It should also be noted there is a possibility that $NaHCO_3$ decomposition to CO_2 and H_2O at the curing temperature can produce pores but as we show below we did not observe fluorescein transport through cured membranes that contained $NaHCO_3$ but were not treated with HCl. Finally, the contact angle of the PDMS films with and without pores remained the same (95 ± 5)° suggesting that the surface energy of the films was not significantly affected by the formation of the pores in the films.

A. 1. Principal pathway of pore formation—In order to establish that evolution of CO_2 from the reaction of $NaHCO_3$ and HCl was the principal reason for the formation of pores and channels within the membrane, we performed flow-experiments with flurosceinate ions on $NaHCO_3$-embedded membranes without treatment with HCl. 50μM fluorescein water solution was placed in one arm of the U-tube while nanopure water was in the other arm. The absorbance of the solution in the right arm was checked every 15 min (Figure 2a). It is evident that there is no flow of fluorescein through this membrane even after 100 minutes. For comparison, the absorbance of fluorescein solution (the blue triangle) in the feed solution is also shown (Figure 2a). Furthermore, the transport of fluorescein through membranes without $NaHCO_3$ but treated with HCl was not observed within the detection limit of our instrument (Figures 2d and 2e). Comparing Figures 2a and 2e with Figures 2b, 2c and 2d (which plot the flow of fluorescein through $NaHCO_3$-containing membranes treated with concentrated HCl), it is appears that the primary contribution to the formation of the through-channels in the PDMS membranes is the release of CO_2 gas from a reaction between $NaHCO_3/Na_2CO_3$ and HCl. Interestingly, the curing of the PDMS at 90 °C did not form through-channels in the membranes suggesting that the reaction of $NaHCO_3/Na_2CO_3$ and HCl is required for the formation of through-channels in the membranes.

A. 2. Electron microscopic evidence of the presence of pores—Scanning electron microscopy (SEM) was used to obtain images of the pores in the PDMS membranes and ascertain their morphologies. Figure 3 shows secondary scanning electron image of the cross-section of a porous membrane soaked in GNPs. Many pores are clearly see in Figures 3a and 3b. The size of those pores varies between <500 nm and 15μm, which are circled by blue and green circles respectively. However, from these images we cannot rule out the presence of pores with diameters smaller than the detection limit of our instrument (~50 nm). Figures 3c and 3d show the surface and cross-sectional images of a typical membrane. These figures suggest that the pore channels are not uni-axial but probably are tortuous in various directions and possibly possess a three-dimensional pore system. These membranes, therefore, appear to contain channels of varying dimensions along their length in a three-dimensional morphology. Another strong evidence of the porosity of the membrane came

from Energy Dispersive X-ray (EDX) analysis. A PDMS membrane was soaked in GNPs (diameter ~ 13 nm) solution followed by thorough washing in water and then was cracked in liquid nitrogen. A thin conductive carbon coating was then applied to the film. The presence of Au element signal in the EDX spectrum inside of the pores confirmed that GNPs penetrated the membrane (Figure 4). Some pores, however, did not show Au in the EDX analysis suggesting that not all of the pores and caves are accessible to GNPs (Figure 2S). That is, some pores are accessible for NPs permeation whereas other pores are "dead–end". We also performed fluorescence microscopy analysis on the membranes soaked in a nile-red (which has a red emission) containing polystyrene nanoparticles of particle diameter of ~240 nm. The membranes containing $NaHCO_3$ and treated with HCl showed a strong red emission from the membranes (Figure 5a), whereas the fluorescent intensity for membranes that did not contain $NaHCO_3$ was insignificant (Figure 5b). These results again indicated that the films with $NaHCO_3$ and treated with HCl produced pores that were accessible to nanoparticles.

A. 3. Proposed mechansim of the porous PDMS membrane—Based on the above experiments, we propose a mechansim of pore formation in the PDMS films that contained $NaHCO_3$ and were treated with HCl (Figure 6). Following soaking in an concentrated HCl solution, porous membranes were formed that contained through channels from one face of the membrane to the other. This argument was supported by our experiment results: Thermally cured membranes but without acid treatment did not show transport of fluorescein dye through the membrane even after three days. However, soaking of this membrane in an acid solution led to linear increase in fluorescein transport through the membrane with time. These results clearly support our argument that the through channels were predominantly formed during acid treatment of $NaHCO_3$ conatining films. Green dots in Figures 6c and 6d represent the mouth of the open channels which are formed after soaking the membranes in the acid. The reaction between sodium bicarbonate and hydrochloric acid released CO_2 which helped in the generation and expansion of the pores and formation of channels. All the pores in the film also contained a signal from sodium element which is attributed to either trapped/unreacted sodium bicarbonate/sodium carbonate (brown dots, Figures 6b, c, d) or sodium chloride (red dots, a reaction by-product between HCl and $NaHCO_3$ or Na_2CO_3, Figures 6b). Incubation of the membranes with gold nanoparticles showed gold element signal in the EDX analysis in many pores, however, some pores did not show gold element signal in the EDX spectrum suggesting that not all of the pores are accessible to GNPs (dead pores in Figures 6 b, c, d). Other channels are accessible to the molecules/particles (shown by the pink lines, Figure 6d). The "inaccessible" pore formation maybe an effect of the size of the $NaHCO_3$ particle; more experiments are however needed to draw an unambiguous conclusion on this. Interestingly, even after thorough rinsing with deionized water, our data shows sodium signal in the EDX spectrum of all membranes we tested. We believe this is due to residue of sodium containing species (Na_2CO_3 and/or NaCl).

B. Flow Measurements

We performed transportation studies through porous PDMS membranes to determine if the pores within the PDMS membranes are truly passable to small molecules and nanoparticles. For these experiments, a $NaHCO_3$/HCl treated PDMS film of 50 μm thickness was sandwiched between two halves of a U-tube as shown in Figure 3S. In the first study, fluorescent sodium flurosceinate, which is readily detectable by UV-Vis spectroscopy, was used as a molecular probe for permeation experiments. Since the fluorescein molecule is much smaller than the pore size, this experiment gave a quick proof-of-concept for our hypothesis that the transport rate can be controlled using mechanical stretching of the membrane. The presence of open channels was also affirmed in our second study by

measuring the ionic conductivity across the membrane when both arms of the U-tube are filled with 5% (w/w) NaCl solution. In the third study, 240 nm fluorescent polystyrene particles were used to determine the effect of mechanical stress on the transport properties of micro-particles through porous PDMS membranes.

B.1. Transport and effect of mechanical stress on transport rate of fluorescein molecules—10 mL of 10 μM solution of the flurosceinate and 10 mL pure water were added into the right and left arms of the U-tube, respectively. The chemical potential generated due to the concentration gradient allowed the flurosceinate ions to pass through the pores into the water arm. This is possible only if the PDMS membranes contained pores that opened all the way through the membrane. Aliquots of the solution from the water arm were taken at regular time intervals for the collection of UV-Vis absorption spectra. Figure 3S also provides visual proof of the flow of fluorescein from the higher concentration arm to the other arm. Figure 2b shows the UV-Vis spectra collected over a period of 100 min through an unstretched membrane that contained 12.5% of $NaHCO_3$ and was treated with HCl. It can be clearly seen from the increase in the absorbance that the amount of fluorescein increases with time, indicating that the PDMS membrane does have channels that allow the flow of the fluorescent molecules. The control experiments with membranes that did not contain any $NaHCO_3$ showed an insignificant measurable fluorescein transport even after 70 minutes (Figures 2a and 2d). These results support our argument that the PDMS films after $NaHCO_3$/HCl treatment contained pores in them and that molecules can pass through them. Changing the location on the same PDMS membrane or varying the amount of $NaHCO_3$ (7.5%, 17.5%) embedded in the PDMS films provided similar results. It is possible that increase in $NaHCO_3$ concentration did not increase the porosity of the membrane and that with increased $NaHCO_3$ present in the films, the evolution of larger amount of CO_2 and water generated released through the pores which were already present in the films without significantly affecting the membrane morphology and porosity.

Since PDMS is flexible, we manually stretched the above membrane by approximately 10% (± 2%) and conducted the fluorescein transport experiments under the same conditions. The stretch percentage was determined by measuring the radius of the stretched portion of the membrane before and after the release of mechanical pressure. The mechanical stretching influenced the pore dimensions which in turn influenced the flow rate of fluorescein. The changes in the fluorescein electronic absorption spectra was detected and quantified by the absorbance as a function of time. Figure 6c plots the absorbance of fluorescein through the stretched membrane over a period of 100 min. Following stretching of the membrane, we found that the transport rate through the membrane was increased from 2 nmole/cm^2-min to 5.6 nmole/cm^2-min (Figure 2d). This represents about 2.8 times increase in the transport rate for a stretched membrane compared to that for an unstretched membrane under the same conditions. One point to be noted here is the apparent static response of the curves at some time intervals (e.g., at 30 min and 40 min). One of the possible reasons for this stagnation could be the tortuosity of the channel through which these molecules move. It is well-known that the presence of tortuosity in the membranes affects the diffusion through it.[36] This effect will be strong at bends and curves, particularly when the bends/curves have smaller dimensions than the rest of the channel. The reduced dimensions will result in greater interparticle collisions and collisions with the walls of the channel both of which will impede flow. Other factors that can come into play are the solvent drag, frictional forces, orientation of the molecules and size of the particles. [37, 38] It is clear that a complete discussion of the reasons of flow behavior through the membrane is complicated and beyond the scope of this paper.

In general, the transport flux (J, in mole/s) through channels is given by:[34] $J = -D(\delta C/\delta x)A$, where D is the diffusion coefficient (cm^2/s), δC (mole/cm^3) is concentration

difference between two parts of the U-tubes across the membrane of thickness δx (cm), and A (cm^2) is the cross-section area of the membrane through which transport was measured. Thus, $\delta C/\delta x$ is the concentration gradient which is the driving force for the molecular transport across the membrane. For all the experiments, δC between two halves of the U-tubes was same within each set of experiments. With all other parameters constant, a 10% stretching of the polymer film will decrease the thickness of the membrane by ~18% and can account for ~18% increase in the transport rate (see Supporting Materials, Figure 5S). It, however, cannot alone explain 2.8 times increase in the transport rate of fluorescein observed in our experiments. So, the question is what can cause such an enhanced fluorescein transport after stretching of the membrane? We attribute the observed large increase in the transport rate of fluorescein is primarily due to increase in the overall dimension of the pores along their length With larger pores, the transport rate will be enhanced through the membranes. Increase in the pore size can also affect the value of D because it depends upon the molecular size (M) with respect to the pore diameter (d). When M and d are comparable to one another, then the transport is called as "*hindered*" transport, and the value of D can be considerably smaller than "*normal*" transport ($M/d \ll 1$). In our case, the membranes have pores with varied dimensions along its length as evident from secondary electron analysis (Figure 3). Thus, it is possible that the streching of the membrane especially at the bottleneck along the pore may have changed D of the molecules that contributed to observed increase in the transport rate of the fluorescein molecules. Overall, the enhancement in the transport rate was attributed due to changes in the D values (due to increase in the pore diameter) and increase in the thickness of the membrane.

B.2. Transport of NaCl across the PDMS membrane—To further establish if the HCl-treated membranes possess through-pores in them, we tested the conductivity of NaCl solution across a porous membrane held between two halves of the U-tube. Both arms of the U-tube were filled up first with nanopure water and then with a 5% w/w NaCl solution. Since the electrolyte in two arms of U-tube had the same concentration and the same height, the application of an electric field is the only driving force to make the ions pass through the PDMS membrane. Significant difference was detected between ionic conductivities of water and NaCl solution. The conductivity of the NaCl solution was about 3 to 4 orders higher than that of water which confirmed that the PDMS membrane allowed the ions to pass through it; that is, they have open channels spacing from one face of the membrane to other in them (Figure 2f).

B.3. Effect of mechanical stress on transport of fluorescent polystyrene nanoparticles—The flow of fluorescein molecules through the PDMS membranes provided evidence of the existence of pores that run across the membrane and their size malleability. The information from the the molecular transport studies cannot be translated for nanoparticles. We, therefore, conducted similar transport studies with 240 nm fluorescent particles. Figures 7a and 7b plot the fluorescent intensity of the particles that emerge from the membrane against time. We observe from the Figure 7 that the fluorescent polystyrene particles of 240 nm pass through the porous membrane. This implies that the prepared membrane contains some pores with diameter >240 nm. Unlike the case of fluorescein transport, the transport rates for the nanoparticles for the stretched membranes was increased but was found to be much less than that for fluorescein permeation studies. After 120 minutes, ~ 4.3×10^9 (~ 4.5×10^{-8} nmole/cm^2-min) and 6×10^9 (~ 6.3×10^{-8} nmole/cm^2-min) particles passed across to the other side of the unstretched and stretched membranes respectively. This transport rate corresponds to an increase of ~38% after stretching and was ~ 10^8 times smaller than the fluorescein transport rate. The concentration of the nanoparticles was estimated from a calibration curve between the number of particles and emission intensity (Figure 4S). The number of particles per unit volume is provided by

the manufacturer. Since the concentration of fluorescein molecules (10μM) was 10^8 times higher than that of fluoresent particles (0.1pM), these very large differences in the particle and molecular transport rate are attributed to a smaller driving force and a smaller D value (please see below) for nanoparticles than those for molecules. Another factor that should be taken into account for considering the differences in the transport rates is the diffusion coefficient differences between fluorescein and the nanoparticles. For the sake of simplicity, lets assume that the Stoke-Einstein equation is valid for both molecules and particles.[39] They will follow the equation: $D = kT/6\pi\eta r$,[39] where r, k, T, and η represent the dimension of molecules/particles, Boltman's constant, temperature and viscosity of the solution respectively. Since the radius for polystyrene nanoparticles is about 250 times larger than that for molecules, the D value for particles is approximately 250 times smaller than that of molecules. Overall, large differences in the transport rate of the nanoparticles in comparison with the fluorescien molecules is attributed to the differences in the diffusion coefficients and driving force (concentration differences) between fluorescein and nanoparticles. The membranes prepared in our studies are also mechanical strong, and they did not rapture or show apparent degradation after being held in a stretching (10 ± 2)% position within a U-tube for more that 3 days. We believe that these membranes can be used for modulating the transport rate of molecules and particles by simple mechanical stretching. More possibilities exists where the membrane pores are vertically aligned and have uniform pore distribution. These membranes would provide opportunities for tunable transport rate by a simple mechanical stretching mechanism.

Conclusion

A facile, simple and highly reproducible chemical method of generating pores via the expulsion of water and CO_2 gaseous species within cured polydimethylsiloxane films is reported. The proposed method of preparation is simple, inexpensive, and does not involve use of organic solvents. Through our electron and fluorescence microscopic analysis, the pores formed in the membranes appeared to be branched and tortuous. Based on our experimental results, a mechansim for the formation of the pores in the PDMS films was proposed. It was observed that some of the channels were accessible to molecular and nanoparticle transport whereas other pores have dead-ends and are not accessible for the transport of molecules and nanoparticles. The stretched and unstretched membranes show different molecular and nanoparticle flow rates indicating that these membranes could be used to modulate transport rate through a simple mechanical stretching process. This is potentially much easier and less expensive compared to the current techniques for adjusting the membrane pore size or transport rate. Additionally, this membrane could potentially be used as a separation technique of many different molecules and nanoparticles using one membrane by a simple mechanical stretching mechanism.

Supplementary Material

Refer to Web version on PubMed Central for supplementary material.

Acknowledgments

Financial support for this work was provided through the National Science Foundation (P.K.), National Institute of Health (NIH), Materials Technology Center (MTC) and ORDA at SIUC. C.L.G. and J.W. were supported through an NSF-REU and a supplement NSF grant. We thank NSF for a grant (CHE-0959568) for the purchase of FE-SEM. We would like to thank Prof. Matthew McCarroll, Dr. Nan Ding, Dr. Chuanhong Zhou, Mr. Pradeep Rajasekaran, Mr. Rashid Zakeri (Indiana University), Mr. Eddie Umana (Washington University) and Mr. Tahir Karimjee for helpful discussions. We also thank Dr. John Bozzola at the IMAGE center for access to the scanning electron microscope and help in collecting the backscattered electron images.

References

1. Jirage KB, Hulteen JC, Martin CR. Nanotubule-based molecular-filtration membranes. Science. 1997; 278:655–658.
2. Bhown AS, Stroeve P. Micelle-mediated transport of a sparingly soluble drug through nanoporous membranes. Ind. Eng. Chem. Res. 2007; 46:6118–6125.
3. Lee SB, Mitchell DT, Trofin L, Nevanen TK, Soderlund H, Martin CR. Antibody-based bio-nanotube membranes for enantiomeric drug separations. Science. 2002; 296:2198–2200. [PubMed: 12077410]
4. Yang SY, Ryu I, Kim HY, Kim JK, Jang SK, Russell TP. Nanoporous membranes with ultrahigh selectivity and flux for the filtration of viruses. Adv. Mater. 2006; 18:709–712.
5. Shannon MA, Bohn PW, Elimelech M, Georgiadis JG, Marinas BJ, Mayes AM. Science and technology for water purification in the coming decades. Nature. 2008; 452:301–310. [PubMed: 18354474]
6. Kohli P, Harrell CC, Cao ZH, Gasparac R, Tan WH, Martin CR. DNAFunctionalized Nanotube Membranes with Single-Base Mismatch Selectivity. Science. 2004; 305:984–986. [PubMed: 15310896]
7. Harrell CC, Siwy ZS, Martin CR. Conical nanopore membranes: Controlling the nanopore shape. Small. 2006; 2:194–198. [PubMed: 17193019]
8. Howorka S, Siwy ZS. Nanopore analytics: sensing of single molecules. Chem. Soc. Rev. 2009; 38:2360–2384. [PubMed: 19623355]
9. Adhikari B, Majumdar S. Polymers in sensor applications. Prog. Polym. Sci. 2004; 29:699–766.
10. Arora P, Zhang Z. Battery Separators. Chem. Rev. 2004; 104:4419–4462. [PubMed: 15669158]
11. Sirkar KK, Shanbhag PV, Kovvali AS. Membrane in a Reactor: A Functional Perspective. Ind. Eng. Chem. Res. 1999; 38:3715–3737.
12. Li QF, He RH, Jensen JO, Bjerrum NJ. Approaches and recent development of polymer electrolyte membranes for fuel cells operating above 100° C. Chem. Mater. 2003; 15:4896–4915.
13. Yan X, Liu G, Dickey M, Willson GC. Preparation of porous polymer membranes using nano- or micro-pillar arrays as templates. Polymer. 2004; 45:8469–8474.
14. Yan F, Goedel WA. Polymer Membranes with Two-Dimensionally Arranged Pores Derived from Monolayers of Silica Particles. Chem. Mater. 2004; 16:1622–1626.
15. Zhang S, Zhou S, You B, Wu L. Fabrication of Ordered Porous Polymer Film via a One-Step Strategy and Its Formation Mechanism. Macromolecules. 2009; 42:3591–3597.
16. Chen W, Wu JS, Xia XH. Porous Anodic Alumina with Continuously Manipulated Pore/Cell Size. ACS Nano. 2008; 2:959–965. [PubMed: 19206493]
17. Fletcher BL, Retterer ST, McKnight TE, Melechko AV, Fowlkes JD, Simpson ML, Doktycz MJ. Actuatable Membranes Based on Polypyrrole-Coated Vertically Aligned Carbon Nanofibers. ACS Nano. 2008; 2:247–254. [PubMed: 19206624]
18. Akthakul A, Hochbaum AI, Stellaci F, Mayes AM. Size fractionation of metal nanoparticles by membrane filtration. Adv. Mater. 2005; 17:532–535.
19. Chun KY, Mafé S, Ramírez P, Stroeve P. Protein transport through gold-coated, charged nanopores: Effects of applied voltage. Chemical and Physical Letters. 2006; 418:557–560.
20. Ku J, Stroeve P. Protein Diffusion in Charged Nanotubes: "On-Off" Behavior of Molecular Transport. Langmuir. 2004; 20:2030–2032. [PubMed: 15801478]
21. Lee SB, Martin CR. Electromodulated Molecular Transport in Gold-Nanotube Membranes. J. Am. Chem. Soc. 2002; 124:11850–11851. [PubMed: 12358519]
22. Yu S, Lee SB, Martin CR. Electrophoretic Protein Transport in Gold Nanotube Membranes. Anal. Chem. 2003; 75:1239–1244. [PubMed: 12659181]
23. Siwy ZS, Howorka S. Engineered voltage-responsive nanopores. Chemical Society Reviews. 2010; 39:1115–1132. [PubMed: 20179828]
24. Siwy ZS. Ion-current rectification in nanopores and nanotubes with broken symmetry. Advanced Functional Materials. 2006; 16:735–746.

25. Li S, Li J, Wang K, Wang C, X J, C H, Xia X, Huo Q. A Nanochannel Array- Based Electrochemical Device for Quantitative Label-free DNA Analysis. ACS Nano. 2010; 4:6417–6424. [PubMed: 20958077]
26. Chen W, W Z, Xia X, Xu J, Chen H. Anomalous Diffusion of Electrically Neutral Molecules in Charged Nanochannels. Angew. Chem. 2010; 49:7943–7947. [PubMed: 20845341]
27. McDonald JC, Whitesides GM. Poly(dimethylsiloxane) as a Material for Fabricating Microfluidic Devices. Acc. Chem. Res. 2002; 35:491–499. [PubMed: 12118988]
28. Song H, Ismagilov RF. Millisecond kinetics on a microfluidic chip using nanoliters of reagents. J. Am. Chem. Soc. 2003; 125:14613–14619. [PubMed: 14624612]
29. Perl A, Reinhoudt DN, Huskens J. Microcontact Printing: Limitations and Achievements. Adv. Mater. 2009; 21:2257–2268.
30. Kobayashi T, Saitoh H, Fujii N, Hoshino Y, Takanashi M. Porous membrane of polydimethylsiloxane by hydrosilylation cure: characteristics of membranes having pores formed by hydrogen foams. J. Appl. Poly. Sci. 1993; 50:971–979.
31. Connal LA, Qiao GG. Preparation of Porous Poly(dimethylsiloxane)-Based Honeycomb Materials with Hierarchal Surface Features and Their Use as Soft Lithography Templates. Adv. Mater. 2006; 18:3024–3028.
32. Juchniewicz M, Stadnik D, Biesiada K, Olszyna A, Chudy M, Brz´ozka Z, Dybko A. Porous crosslinked PDMS-microchannels coatings. Sensors and Actuators B. 2007; 126:68–72.
33. Kellenberger, Christoph R.; Luechinger, Norman A.; Lamprou, Alexandros; Rossier, Michael; Grass, Robert N.; Stark, Wendelin J. Soluble nanoparticles as removable pore templates for the preparation of polymer ultrafiltration membranes. Journal of membrane science. 2012; 387:76–82.
34. Atkins, Peter; de Paula, Julio. Atkin's Physical Chemistry. Ed. 8. Oxford Press; 2006. Chapter 9
35. McFarland AD, Haynes CL, Mirkin CA, Van Duyne RP, Godwin Hilary A. Color my nanoworld. J. Chem. Educ. 2004; 81:544A–544B.
36. Deen WM. Hindered transport of large molecules in liquid-filled pores. AIChE Journal. 1987; 33:1409–1425.
37. Beck RE, Schultz JS. Hindered Diffusion in Microporous Membranes with Known Pore Geometry. Science. 1970; 170:1302–1305. [PubMed: 17829429]
38. Mota M, Texeira JA, Bowen R, Yelshin A. Proceedings of the World Filtration Congress 8. 2000; 1:57–60.
39. Edward JT. Molecular Volumes and the Stokes-Einstein Equation. Journal of Chemical Education 47. 1970; 4:261–270.

Highlights

- Novel process to produce pores in cured polydimethylsiloxane membranes
- CO_2 and H_2O from the reaction of conc. HCl and embedded $NaHCO_3$ create pores in PDMS
- Transport data of ions and nanoparticles through the membranes
- Flexibility of PDMS enables flow modulation through the membrane
- Mechanically stretching increases the flow rate of ions and nanoparticles

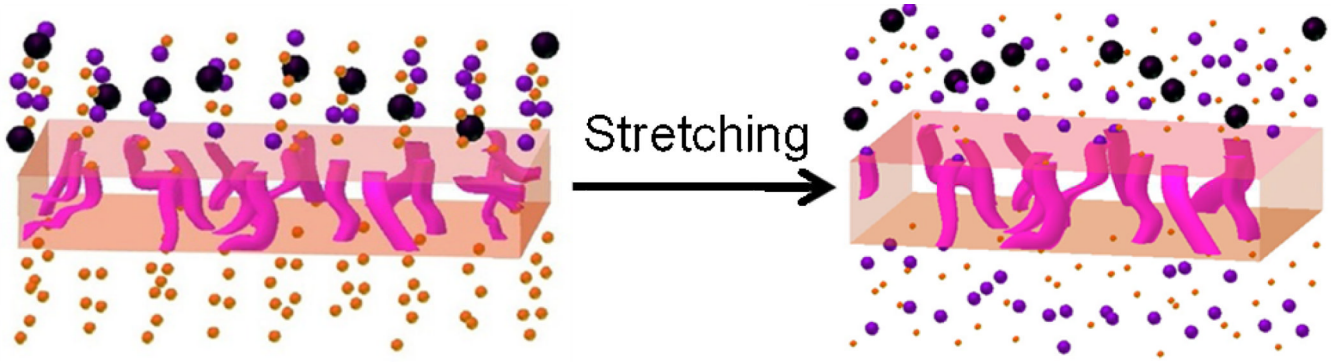

Figure 1.
A schematic diagram of (a) an unstretched and (b) a stretched porous PDMS membrane shows the mechanism of modulation of transport of molecules and particles.

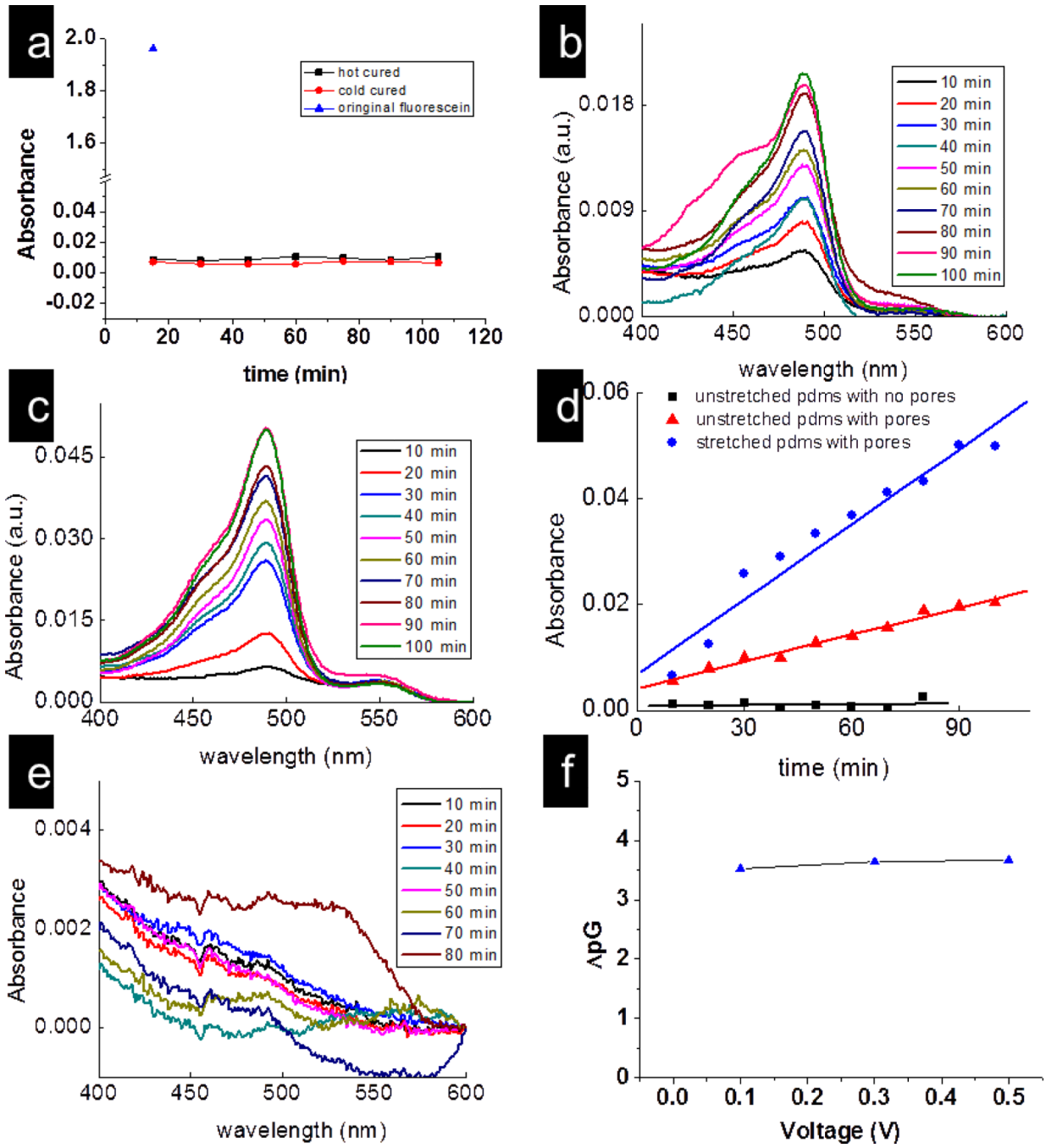

Figure 2.

(a) Plots of absorbance versus time for the fluorescein molecules passed through the hot cured and cold cured PDMS membrane without treated with acid. Plots of absorbance of fluoresceinate versus wavelength for(b) an unstretched; (c) a stretched porous PDMS membrane; and (d) Plot of absorbance of fluorescein at 490 nm versus time for passage of these molecules through stretched (circle); unstretched (triangle) porous PDMS; and through a PDMS film containing no $NaHCO_3$ (square); (e) a PDMS film containing no $NaHCO_3$. (f) Difference between the conductivities of NaCl solution and pure water in the U-tube with porous PDMS membrane, y-axis represents the logarithm of the difference between the two conductivities.

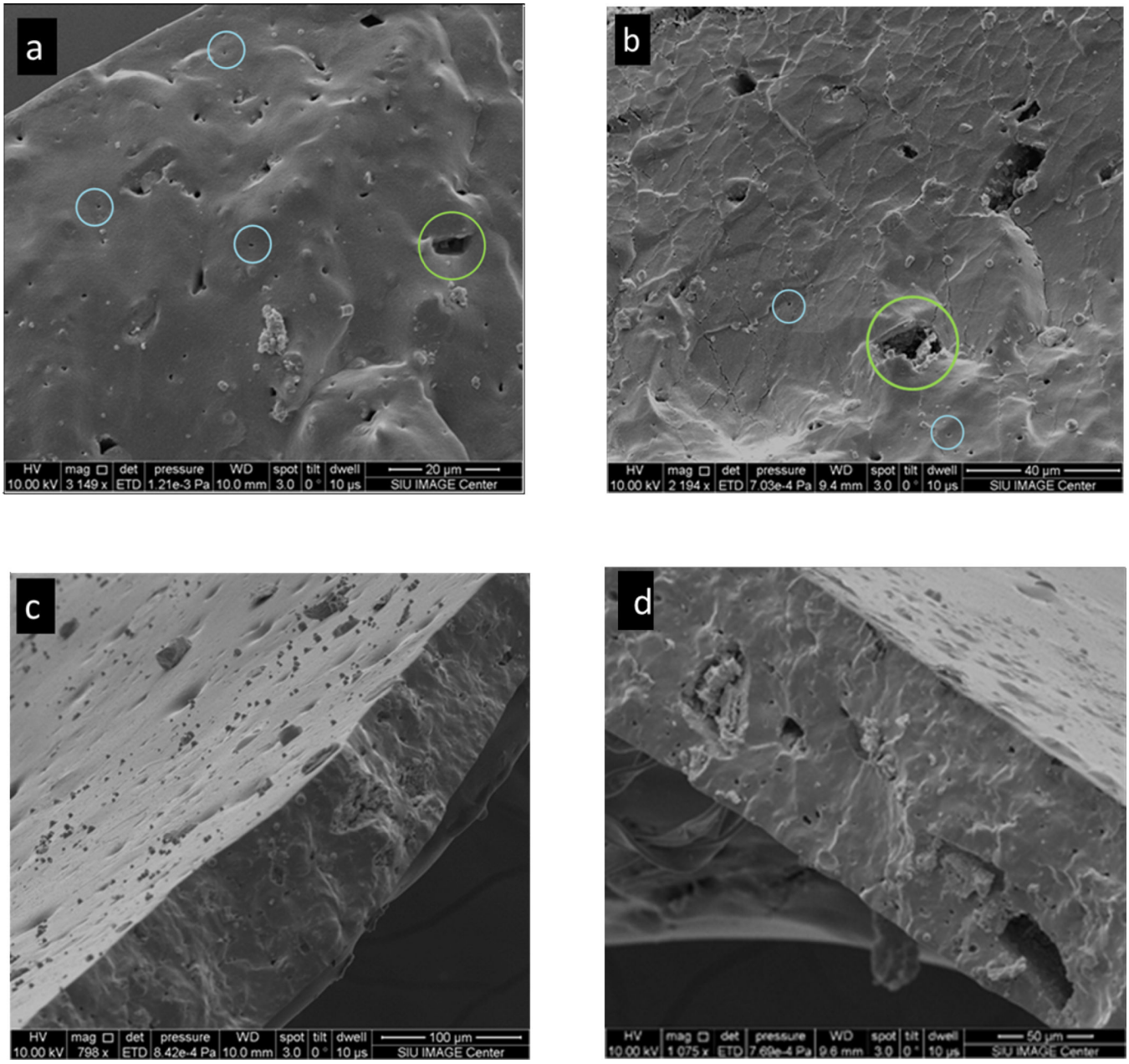

Figure 3.

Secondary electron images of the pore structure after filling the pore channels with gold nanoparticles. (a) and (b)A secondary electron image showing pores on the cross-section of the PDMS membrane. Blue and green denote the large pore and small pores on the cross-section; (c) and (d) a secondary electron image showing the pores on both the cross-section and the surface of the regular PDMS membrane.

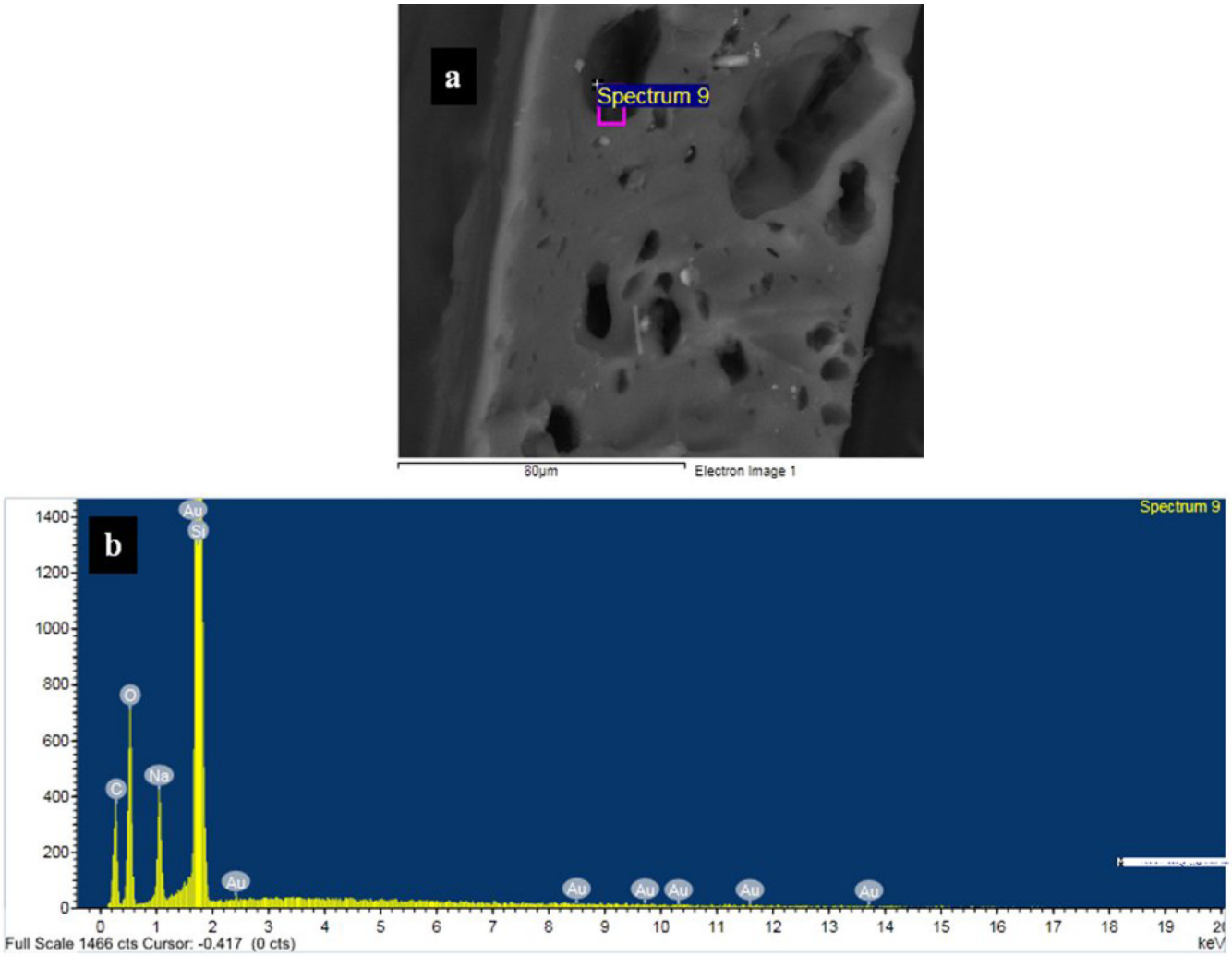

Figure 4.

(a) An BSE (back scattering electrons) of a membrane after it was soaked with GNPs and corresponding EDX analysis of a pore showing the presence of elemental gold along with Si, O, C and Na signal (b).

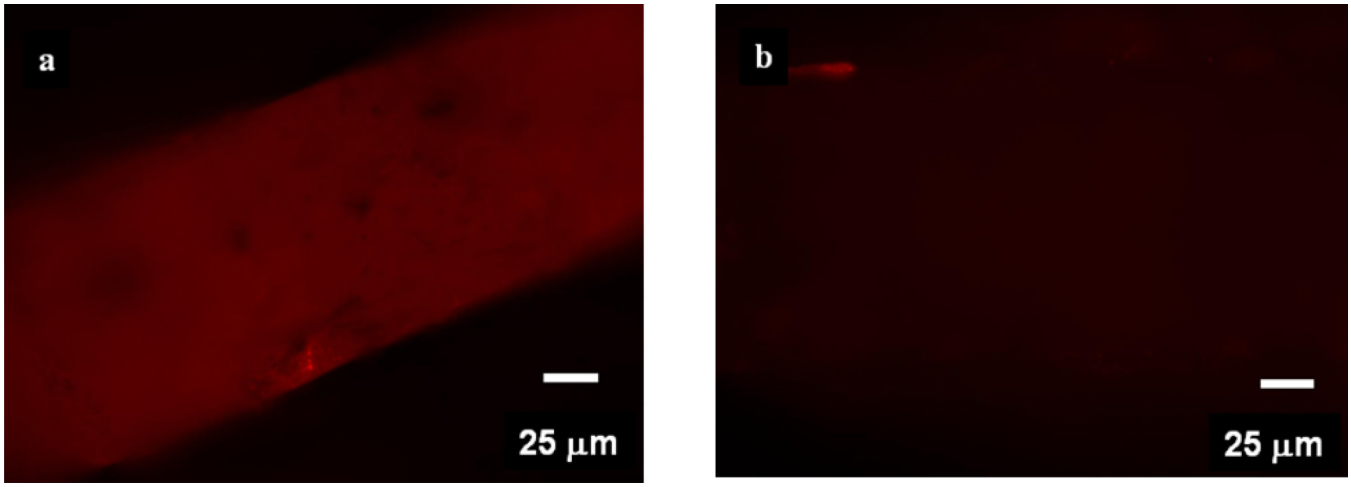

Figure 5.

(a) A fluorescence image of a porous membrane (contained $NaHCO_3$ and was treated with HCl) soaked in a red-nile impregnated 240 nm polystyrene nanoparticles. (b) A fluorescence image of a film that did not contain $NaHCO_3$ and acid treatment but was soaked with polystyrene nanoparticles under the same experimental conditions.

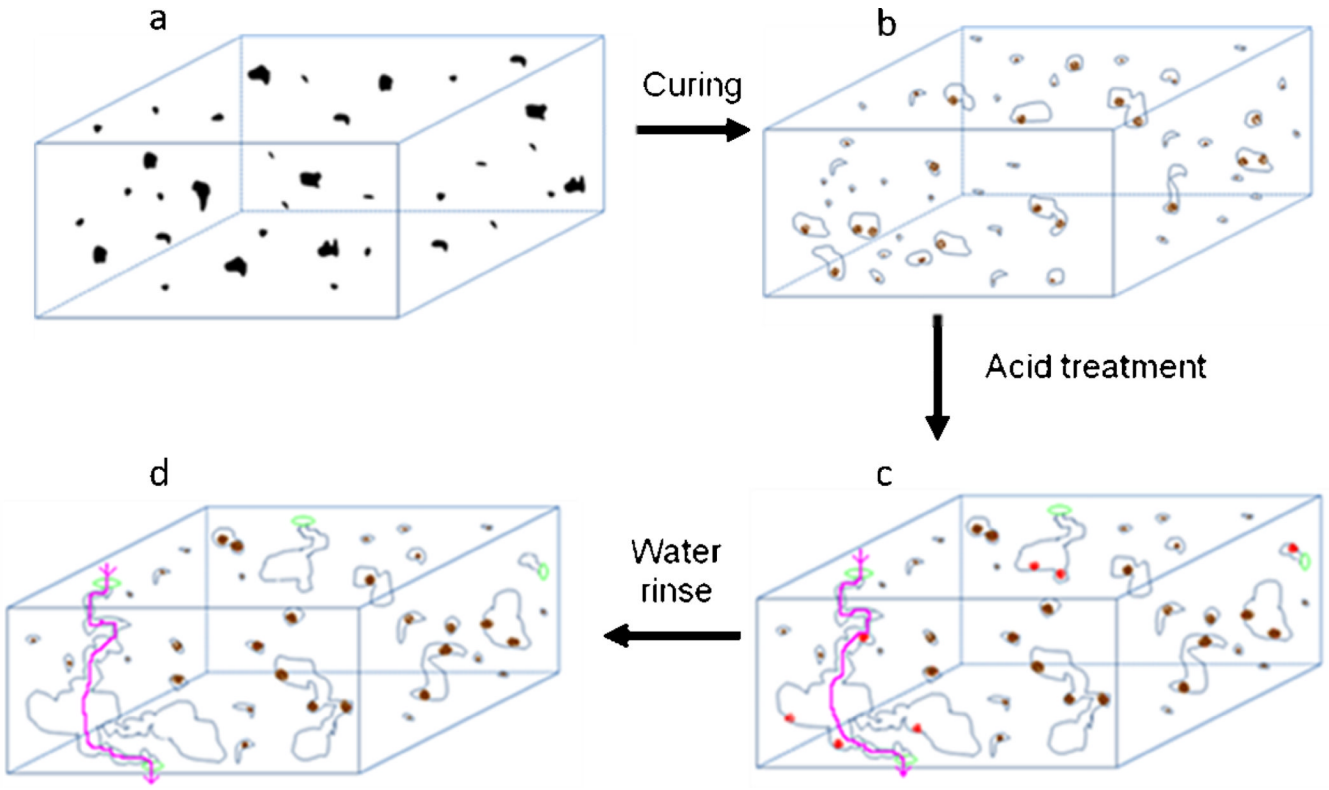

Figure 6.

A proposed mechanism for the formation of the porous PDMS membranes using an *in-situ* chemical reaction that generated gaseous products. Black dots in are sodium bicarbonate particles embedded in the PDMS matrix which on heating decomposed to sodium carbonate (brown dots) along with release of CO_2 gas. Light blue circles which represent pores formed by expanded gas due to reaction between curing. The acid treatment of the membrane increases the porosity of the membrane. Sodium chloride (red dots) was washed away in water. Green circles represent open access of channels made from expanded pores, and pink line denotes a possible channel that passes from one face of the membrane to the other face. Some of sodium carbonate particles were remained trapped in the particles as evident from EDX data.

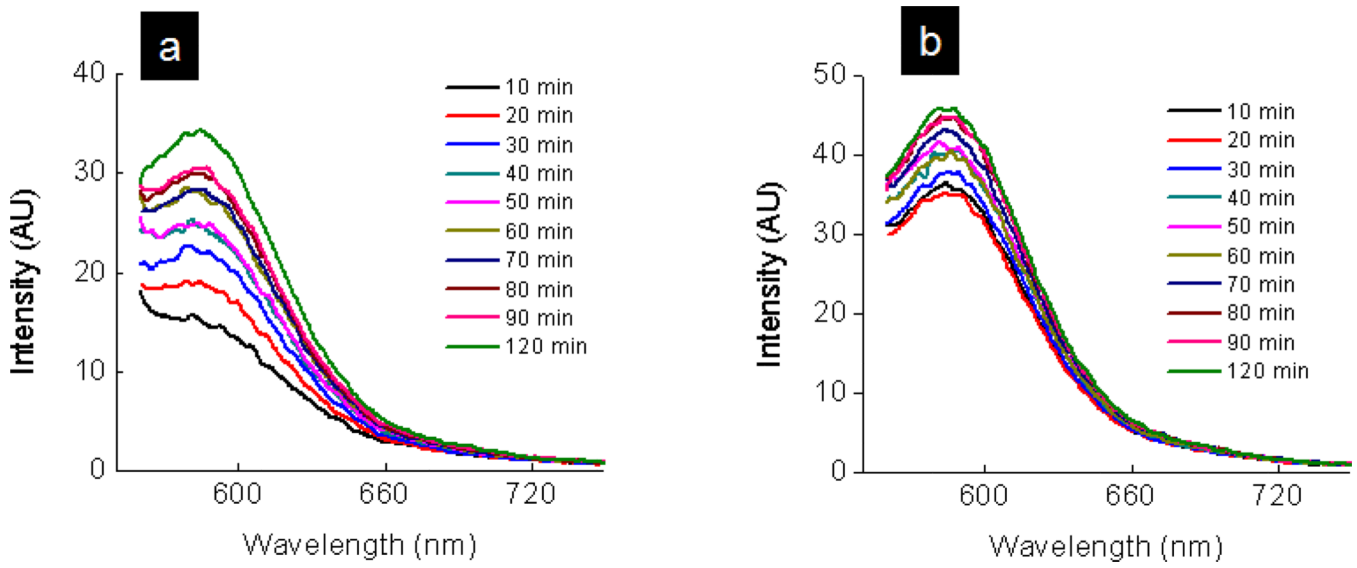

Figure 7.

Plot of fluorescent intensity of 240 nm polystyrene particles versus wavelength for the (a) unstretched membrane (b) stretched membrane shows the passage of polystyrene particles through the porous PDMS membrane.